The Hα Emission of Helium-rich Stars

Ryûzô NAKAJIMA

Astronomical Institute, Faculty of Science,
Tôhoku University, Sendai 980.

(Received July 15, 1981)

The circumstellar gas of helium-rich stars will be trapped in the outer region of stellar magnetosphere where the centrifugal force dominates. Only in rapidly rotating stars, the outer region can contain the gas much enough to emit the observed Hα emission energy flux. As the circumstellar gas corotates with the star, the Hα emission profile becomes very broad and so the emission will appear in the wing of Hα absorption line which originates in the photosphere of star.

Keywords: Helium-rich stars, Hα emission, Stellar Magnetosphere.

§1. Introduction

The principal characteristics of helium-rich stars are that they have spectral types very close to B2V, but with abnormally strong neutral-helium lines whose strength is variable.[1,2] Osmer and Peterson[3] have carried out a spectroscopic investigation of helium-rich stars. They find that helium-rich stars, as a group, have helium abundances comparable to hydrogen by number, order-of-magnitude overabundance of oxygen and nitrogen, and basically normal abundance of carbon, silicon, magnesium, and alminium. They suggest that helium-rich stars are an extension to higher effective temperatures of the Ap phenomena. Their suggestion has been confirmed by the discovery of variable strong magnetic fields of the order of 10^4 gauss in some of helium-rich stars.[4,5]

Walborn[6] has found that σ Ori E, the helium-rich star discovered first, has broad variable emission at Hα. He has also detected a probable weak emission to the red side of Hα in HD 37017 and HD 64740. Pedersen[2] has confirmed Walborn's observation. Borra and Landstreet[5] note that helium-rich stars with emission at Hα have short periods ($\sim$1 day) and high rotational velocities ($v \sin i \sim 150$ km s^{-1}).

The fact that helium-rich stars are confined to the galactic plane[7] and many of them are found in or near the Orion Nebula, suggests that they are very young stars. Especially, the fact that three (σ Ori E, HD 37017, HD 37776) out of four stars with the Hα emission is found in the Orion suggests that the presence of the Hα emission has some connection with their age. Namely, we

may consider that the gas which had existed around the star in the process of star formation was trapped by stellar magnetic field and has continued to exist till now. Groote, Hunger and Schults[8] have observed variable IR excess in helium-rich stars. This observation confirms the above consideration.

As gas is almost completely ionized near early B type stars, it may be possible that the gas is trapped around the star by strong magnetic field. In section 2, we discuss the trapping region for gas and its shape. As we assume that the gas density distribution departs from a hydrostatic equilibrium density distribution, the gas will flow along magnetic field lines till it reaches the hydrostatic equilibrium. This flow and outward diffusion across magnetic field lines are discussed in section 3. In section 4, the Hα emission profiles are calculated for the corotating circumstellar gas.

In this model, the Hα line profiles of helium-rich stars with Hα emission are interpreted as the superposition of the Hα emission from the gas which is trapped in the magnetosphere and corotates with the star, and the Hα absorption line which originates in the stellar photosphere.

§2. Trapping Region for Circumstellar Gas

2-1. Magnetic geometry and magnetosphere

Landstreet and Borra[4] and Borra and Landstreet[5] showed that the observed magnetic field variations can be reproduced by a centered oblique dipole rotator model, and estimated its parameters i (the inclination of the rotation axis to the line of sight), β (the inclination of the dipole to rotation axes). They found that HD 37017 and HD 64740 are low obliquity cases. In Ap stars, high and low obliquity cases exist.[9]

Another parameter Bp (the polar field strength) may be estimated by[10]

$$B_{em} = 0.316\ Bp\ \cos(\beta \pm i), \tag{1}$$

where B_{em} is the maximum (minimum) value of the observed magnetic field strengths. We find from equation (1) that $Bp \gtrsim 5\times10^3$ gauss for helium-rich stars for $B_{em} \gtrsim 10^3$ gauss.

While helium-rich stars are located in the region of the H-R diagram where a mass-loss is believed to take place,[11] there is not any observational evidence that B2V stars are losing mass.[12] It has been proposed by Havnes and Conti[13] and Havnes[14] that early type stars with strong magnetic fields have large-scale magnetospheres which consist of closed field lines, if they are not losing mass. In the case of corotating magnetosphere, Havnes[14] obtained the lower limit of its radius,

$$r_{MS} = 6.0 \times 10^{-11} \left[\frac{B_p^2\ r_*^6\ P}{n_p}\right]^{1/7} \quad \text{a.u.}, \tag{2}$$

where r_* is the stellar radius, P, the period of rotation, and n_p, the number density of ionized interstellar gas. For $Bp \gtrsim 5\times10^3$ gauss, $P = 1^d.0$, $n_p = 1$ cm^{-3}, and $r_* = 5R_\odot$, we obtain $r_{MS} \gtrsim 5.3$ a.u. We will show below that the circumstellar gas responsible for the Hα emission can be trapped in the magnetosphere.

2-2. Potential along a magnetic field line

If the gas trapped in the magnetosphere corotates with the star, it is subject to a gravitational force and a centrifugal one in the frame that corotates with the star. Thus, a potential per unit mass for the gas is given by

$$\Phi = -\frac{GM_*}{r_*}\frac{1}{R} - \frac{\Omega_*^2 r_*^2}{2} R^2 \sin^2\alpha \qquad (3)$$

where G is the gravitational constant, M_*, the stellar mass, R, the radial distance in units of r_*, and α, the angle between the rotation axis of the star and the radius vector.

It is worth-while treating the potential along a magnetic field line as the gas moves along it. If the magnetic field is dipolar, the field line satisfies

$$R = L \sin^2\theta, \qquad (4)$$

where θ is the magnetic co-latitude and L is the maximum distance of the field line from the center of the star in units of r_*, which will be used to identify the field line, and α is given by

$$\sin^2\alpha = 1 - (\cos\beta\cos\theta + \sin\beta\sin\theta\cos\varphi)^2, \qquad (5)$$

where φ is the angle between the plane which contains the rotation and dipole axes and the plane which contains any field line (hereafter refer to the latter as φ-plane). From equations (3), (4), and (5), we can obtain the potential along the field line. The results are shown in Figure 1 for $M_* = 9.0M_\odot$, $r_* = 5.0R_\odot$, and $P = 1^d.0$. Figure 1(a) and (b) show that the potential has a central minimum for any field line which extends far enough (L = 2.5). The potential minimum occurs at the magnetic equatorial plane (i.e. θ = 90°) for β = 0° and 90°, and its value decreases with increasing L. The magnetic co-latitude for a potential maximum is given by

$$\sin\theta_{MAX} = \left(\frac{2GM_*}{3\Omega^2 r_*^3}\frac{1}{L^3}\right)^{1/8} \quad (\text{for } \beta = 0°),$$

and

$$\sin\theta_{MAX} = \left(\frac{GM_*}{\Omega^2 r_*^3}\frac{1}{L^3}\right)^{1/6} \quad (\text{for } \beta = 90° \text{ and } \varphi = 90°).$$

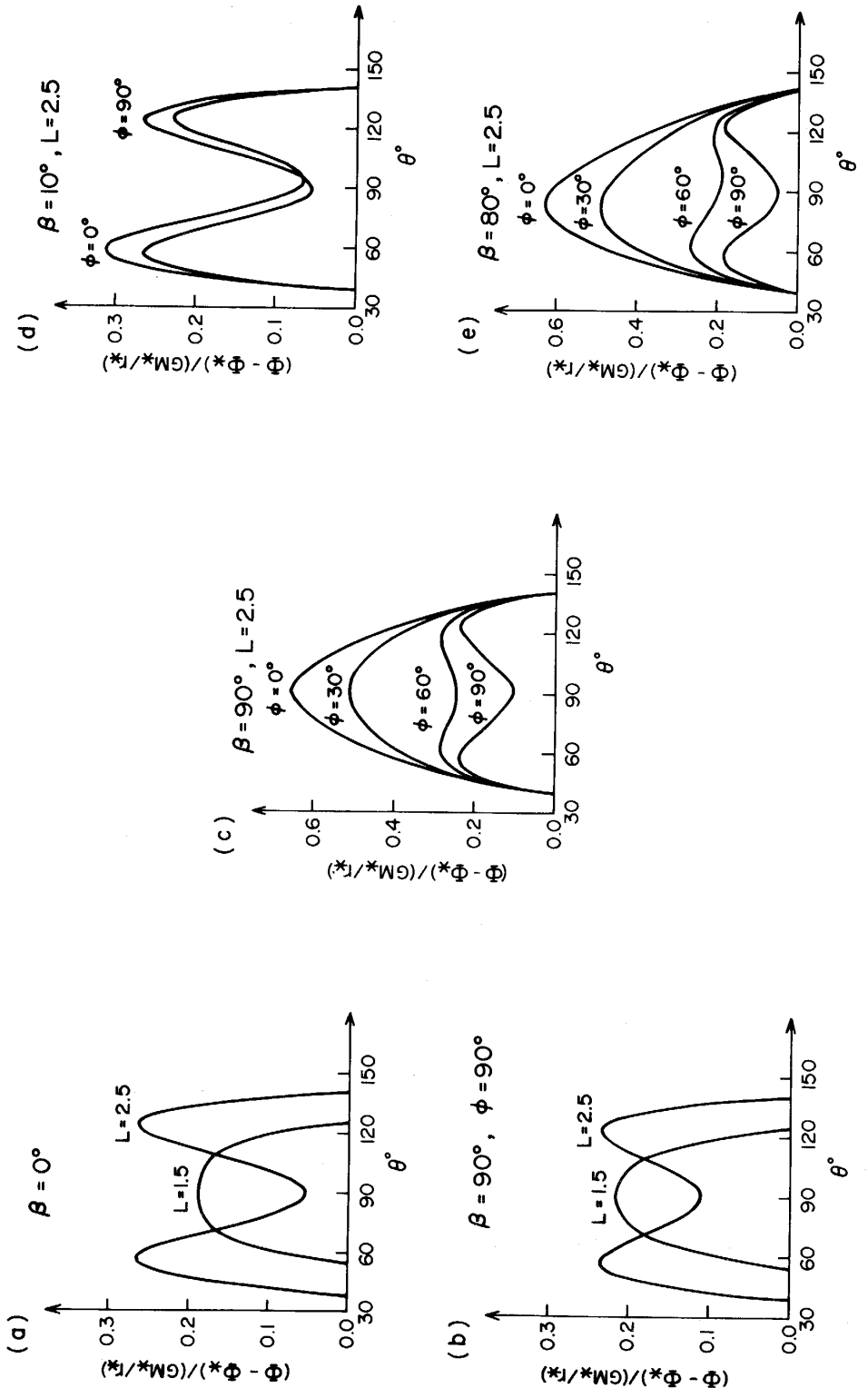

Fig. 1. The potential along field line as a function of magnetic co-latitude. Φ_* stands for the potential at the stellar surface. (see text for details)

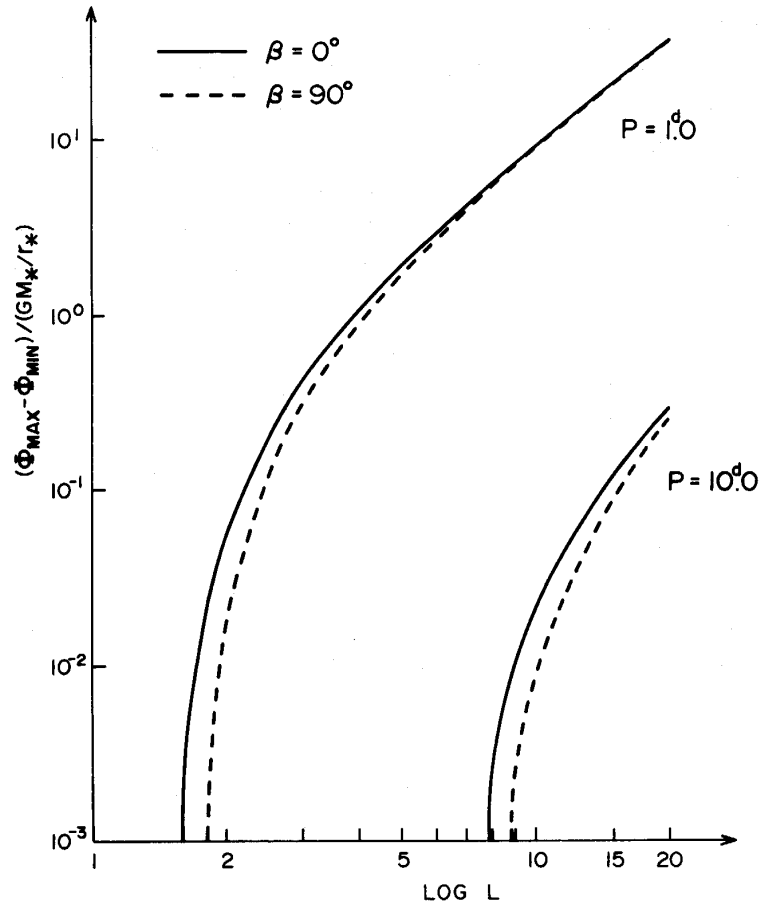

Fig. 2. The potential difference between the maximum and the minimum as a function of L.

Figure 2 shows a potential difference between the maximum and the minimum as a function of L. We find from the figure that the potential difference increases with increasing L, and that a minumum L-value of the field line for which the potential has the minimum increases with increasing P. Figure 1(c) shows, for the case of $\beta = 90°$, the potential for the field line with constant L-value on different φ-planes. We find from the figure that the potential minimum occurs for the field line on the plane with large φ, that is, it occurs near the intersection of the magnetic and rotational equatorial planes. In the case of $\beta = 90°$, the shape of potential does not depend on φ for the field lines with the same L-value. Except for the cases of $\beta = 0°$ and 90°, the situation is very complicated (Figure 1(d) and (e)). The same situation is also found in comparison of Figure 1(e) and (c). In spite of the complicated appearance, however, we find that the potential minimum occurs near the intersection of the magnetic and rotational equatorial planes.

On the field line with potential minimum, the field-aligned component of gravitational force balances the corresponding component of centrifugal force at the potential maximum. In the cases of $\beta = 0°$ and 90°, this force balance distance is given by[15,16]

$$R_{fb}^3 = \frac{2GM_*}{\Omega^2 r_*^3} \frac{1}{3 \sin^2 \alpha}, \qquad (6\text{-a})$$

and

$$R_{fb}^3 = \frac{2GM_*}{\Omega^2 r_*^3} \frac{1}{3 \sin^2 \alpha - 1}, \qquad (6\text{-b})$$

respectively, where R_{fb} is measured in units of r_*. The force balance distance

is independent of the magnetic field strength and forms a surface of revolution around the rotation axis of star. In other words, the field line with potential minimum passes through this force balance surface. Figure 3 shows the force balance distance on the plane which contains the rotation axis of star. We find from the figure that the force balance surface becomes more distant from the star with increasing P. This means that the minimum L-value of field line with potential minimum increases with increasing P and has been already shown in Figure 2. In the case of $\beta = 90°$, the force balance point does not occur at the angle smaller than 35.2°, and Figure 1(c) shows this. It is convenient to separate the magnetosphere into an inner region in which the gravitational force dominates, and an outer region in which the centrifugal force deminates.

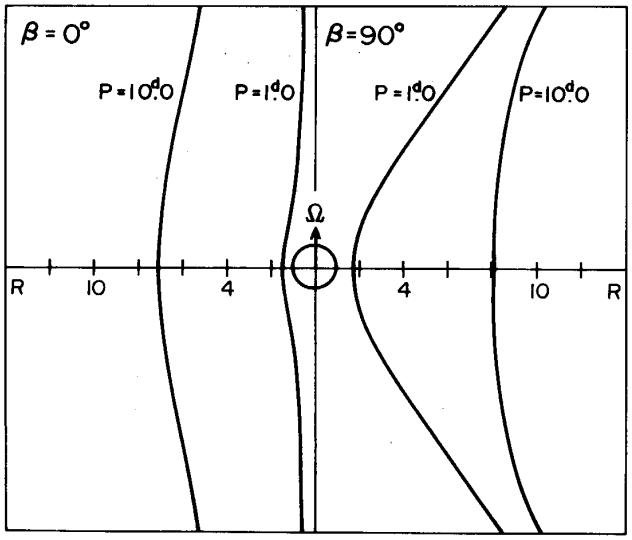

Fig. 3. The loci of the force balance distance on the plane which contains the rotation axis of star.

The outer region surrounds the inner region like as a well of potential. If the kinetic energy of gas were less than a depth of the well in corotating frame, the gas could not get out of the well. Therefore, the outer region would be a trapping region for such gas. In the trapping region, the gas will be thrown out to those parts of the field lines which are the most distant from the rotation axis. An electromagnetic force will exert enough force on the gas to provide the required centripetal acceleration. The pressure scale height of gas along field lines in the trapping region is approximately given by, near the magnetic equatorial plane,

$$H = \sqrt{\frac{2kT}{3\, m_p\, \Omega^2}} \qquad (\text{for } \beta = 0°), \tag{7-a}$$

and

$$H = \sqrt{\frac{4kT}{m_p\, \Omega^2}} \qquad (\text{for } \beta = 90° \text{ and } \varphi = 90°), \tag{7-b}$$

where k is the Boltzmann's constant, T, the temperature of gas, and m_p, the proton mass. Note that the pressure scale height is independent of the radial distance. Considering that the potential minimum, as described above, occurs near the intersection of the magnetic and rotational equatorial planes, the gas will distribute like as the Saturn's ring in the case of small β and like as slabs on both sides of the star in the case of large β.

§3. Circumstellar Gas Trapped in the Outer Region

3-1. Critical density

The magnetic field cannot contain the gas having a higher energy density than the local magnetic energy density. Thus, there is a critical density of gas which can corotate with the magnetosphere at a given distance. We may estimate the critical density on the rotational equatorial plane by equating the magnetic and corotational kinetic energy densities,

$$\frac{B^2}{8\pi} = \frac{1}{2} m_p n_c (r\Omega)^2 , \tag{8}$$

where n_c is the critical density of gas and r is the radial distance. Assuming the magnetic field to be dipolar, we find from equation (8)

$$n_c = 9.8 \times 10^{-2} \frac{B_p^2}{\Omega^2 L^8} \text{ cm}^{-3}. \tag{9}$$

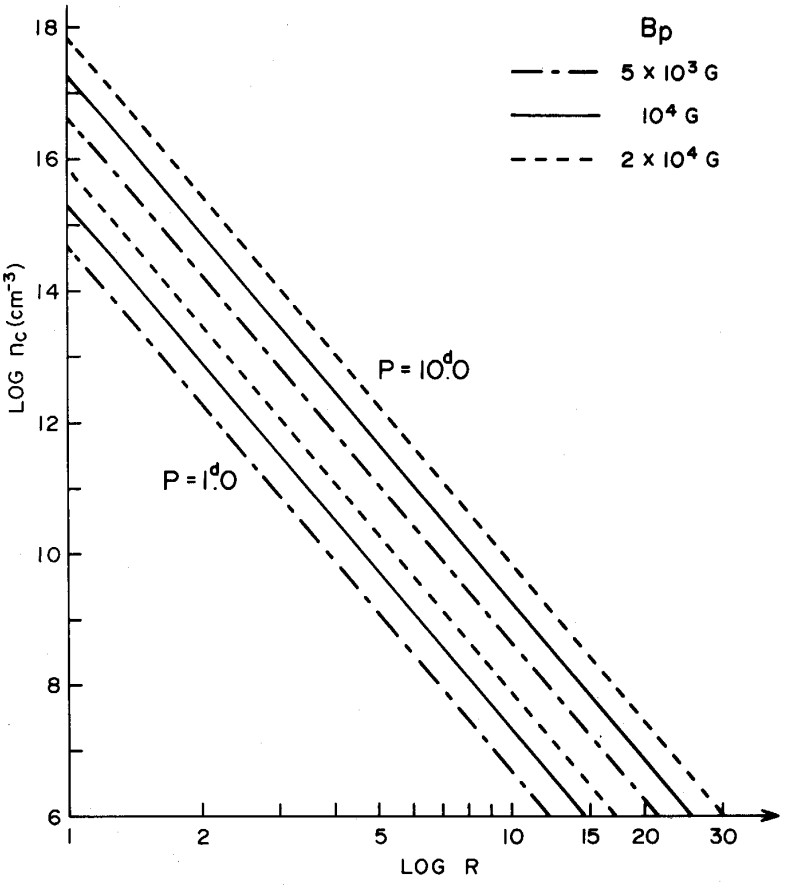

Fig. 4. The critical density distribution on the rotational equatorial plane as a function of R.

Figure 4 shows the critical density distribution for different Bp as a function of R. While, at a given distance, the critical density for $P = 1^d.0$ is less than that for $P = 10^d.0$, its maximum value in the outer region is larger than that for $P = 10^d.0$ as the outer region is more distant from the star for $P = 10^d.0$ than for $P = 1^d.0$. In the case of $\beta = 90°$, the maximum critical density in the outer region is $\sim 10^{13}\,\text{cm}^{-3}$ for $P = 1^d.0$, and $\sim 10^{10}\,\text{cm}^{-3}$ for $P = 10^d.0$ (cf. Fig. 3). If the gas density exceeds the critical density at any point, field lines open and so the gas density becomes far less.

3-2. Leakage of gas from the trapping region

In this model, we suppose that the gas density distribution in the trapping region departs from a hydrostatic equilibrium one. Thus, the gas will flow along field lines till it reaches the hydrostatic equilibrium. In the absence of mass loss, this relaxation time may be estimated by $t_e \sim r_* L/u$ where $r_* L$ is the length of field line and u is the velocity of sound. For $T = 10^4$ K, we find $t_e \sim 10$ day.

However, the flow must get over the potential barrier. If the density distribution of the flow is nearly that of the hydrostatic equilibrium, it will be

$$n = n_e \exp\left\{-\frac{m_p\,(\Phi - \Phi_{MIN})}{2kT}\right\}$$

for the flow from the outer to inner regions, where n_e and Φ_{MIN} are the density and the potential at the potential minimum or the maximum distance of field line, respectively. This equation gives the density which decreases with decreasing co-latitude. For $\beta = 90°$, $L = 2.5$, $T = 10^4$K, and $n_e = 10^{12}$ cm^{-3}, we obtain $n = 3.7 \times 10^{-9}$cm^{-3} at $\theta = 79.9°$, and so the mean collision time between gas particles is $t_c = 11.35\ T^{3/2}/(n \ln \Lambda) \sim 10^7$ year with $\ln \Lambda \sim 10$, which is as long as the life time of B type stars. The ratio of the lengths of field line ℓ_r/ℓ_t is about 0.45, where ℓ_r and ℓ_t are the lengths of field line from $\theta = 90°$ to $\theta = 79.9°$ and to θ_{MAX}. This means that the flow does not occur within the life time of the star. We also find the same result for the flow from the stellar atmosphere to the outer region. Therefore, we may conclude that the flow along field lines is negligible except for the field lines on which the potential difference is small.

Next, let us consider the diffusion across strong magnetic field which originates from a finite resistivity. Outward diffusion velocity for this process is[17]

$$v_\perp = -\frac{\eta}{B^2}\,(\nabla p + n\, m_p \nabla \Phi) \quad \text{cm s}^{-1}, \tag{10}$$

where η, the resistivity, is given by

$$\eta = 1.29 \times 10^{13}\,\frac{\ln \Lambda}{T^{3/2}}$$

with $\ln \Lambda \sim 10$. Assuming that the gas is isothermal, and that the gas density distribution is the critical density distribution (Eq. (9)), we obtain

$$\nabla p = -1.18 \times 10^{-7}\,\frac{1}{L^9}\,,$$

and

$$n\, m_p \nabla \Phi = -5.71 \times 10^{-6}\,\frac{1}{L^7}\,,$$

for $B_p = 10^4$ gauss, $P = 1^d.0$, and $T = 10^4$ K. Thus, equation (10) is reduced to

$$|v_\perp| = 2.95 \times 10^{-5} \frac{1}{L} \text{ cm s}^{-1} \tag{11}$$

if we neglect the pressure force. Then, we find that it takes $t \sim r_*/v_\perp \sim 10^8$ year so that the gas diffuses one stellar radius. This time is longer than the life time of B type stars. Even if the gas density decreases more slowly with radial distance than that given by equation (9), the diffusion time becomes only longer. Therefore, we can neglect also the diffusion across magnetic field lines.

§4. Hα Emission from the Circumstellar Gas

If a star is extremely helium-rich, its atmosphere is certainly different from that of normal composition. However, Chadeau[18] has noticed that the continuous energy distribution of the emergent flux in the visible region depends little on the helium composition as long as the ratio n_H/n_{He} exceeds 1.5, though the discontinuities at λ3647(HI) and λ3422(HeI) depend on this ratio. In the following, for simplicity, we use the emergent flux of normal composition.

It is worth-while considering the Hα emission for critical gas density distribution (Eq. (9)), though the magnetic field is severely distorted. In this case, Hα energy emitted reaches its maximum. If we assume that the circumstellar gas is fully ionized, optically thin at Hα, and isothermal, then the total energy emitted at Hα per unit time is approximately given by (see Fig. 5)

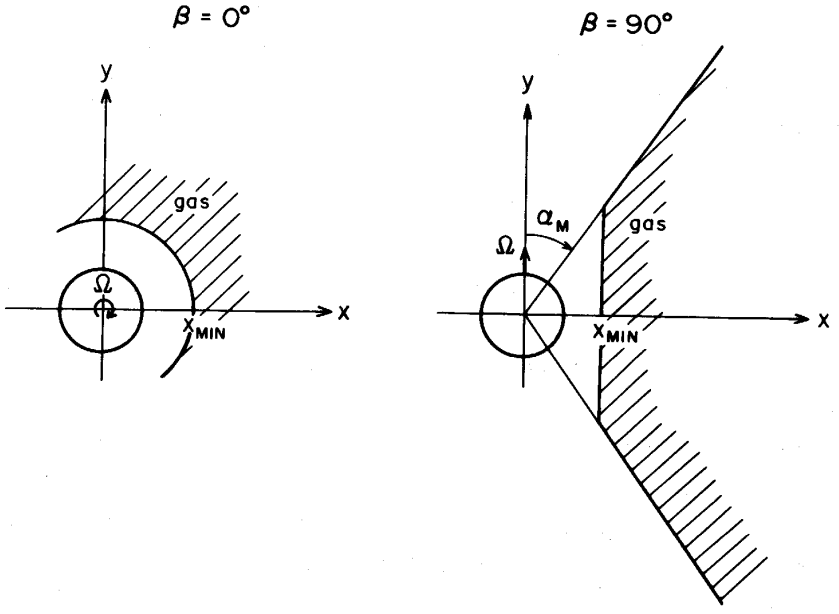

Fig. 5. Schematic diagram of the circumstellar gas trapped in the magnetosphere (hatched area). In the case of $\beta = 90°$, the trapping region is approximated by the straight lines.

$$E_{tot} = \int_{-\infty}^{+\infty}\int_{r_{MIN}}^{+\infty} 4\pi j_{H\alpha}\{n_c e^{-(\frac{h}{H})^2}\}^2\, 2\pi r\, dr\, dh \quad (\text{for } \beta = 0°), \tag{12-a}$$

where $r = \sqrt{(x^2 + y^2)}$ and h is the height from magnetic equatorial plane, and

$$E_{tot} = 4\int_{r_{MIN}}^{+\infty}\int_{0}^{\frac{x}{\tan\alpha_M}}\int_{-\infty}^{+\infty} 4\pi j_{H\alpha}\{n_c' e^{-(\frac{h}{H})^2}\}^2\, dh\, dy\, dx \quad (\text{for } \beta = 90°), \tag{12-b}$$

where $n_c' = n_c/\sin^2\alpha$ and $j_{H\alpha}$ is an emission coefficient (erg cm^{-3} s^{-1} $sterad^{-1}$) calculated by Osterbrock.[19] For $Bp = 10^4$ gauss and $T = 10^4$ K, we obtain from equations (12-a) and (12-b)

$$E_{tot} = \begin{cases} 3.3 \times 10^{35} \text{ erg s}^{-1} & (\text{for } \beta = 0°) \\ 3.1 \times 10^{34} \text{ erg s}^{-1} & (\text{for } \beta = 90°) \end{cases}$$

for $P = 1\overset{d}{.}0$, and

$$E_{tot} = \begin{cases} 1.7 \times 10^{30} \text{ erg s}^{-1} & (\text{for } \beta = 0°) \\ 5.1 \times 10^{29} \text{ erg s}^{-1} & (\text{for } \beta = 90°) \end{cases}$$

for $P = 10\overset{d}{.}0$. We find that the total energy for $P = 10\overset{d}{.}0$ is much smaller than that for $P = 1\overset{d}{.}0$. This means that the emission energy from the gas decreases with increasing P. On the other hand, continuous energy near Hα emitted from the stellar surface is[20]

$$E_c = 2.0 \times 10^{32} \text{ erg s}^{-1} \text{ Å}^{-1}.$$

Thus, the equivalent width of the total emission for $P = 10\overset{d}{.}0$ is $\sim 8 \times 10^{-3}$Å, and is negligible.

The profile of Hα emission may be easily obtained since the corotational velocity of gas considerably exceeds the thermal velocity of gas. In this case, we can suppose that the radiation within the wavelength interval $\Delta\lambda_{th} = 2\mathcal{V}_{th}\lambda/c$ contributes to the radiation of wavelength λ, where $\mathcal{V}_{th}$ is the mean thermal velocity of gas and c is the speed of light.[21] In the case that we see the star from the direction perpendicular to the rotation axis, we obtain

$$E_{H\alpha}(\lambda) = \begin{cases} 2\int_{\sqrt{r_{MIN}^2 - x^2}}^{+\infty}\int_{-\infty}^{+\infty} 4\pi j_{H\alpha}\{n_c e^{-(\frac{h}{H})^2}\}^2\, dh\, dy\, \Delta x & (\text{for } r_* \leqq x \leqq x_{MIN}) \\ 2\int_{0}^{+\infty}\int_{-\infty}^{+\infty} 4\pi j_{H\alpha}\{n_c e^{-(\frac{h}{H})^2}\}^2\, dh\, dy\, \Delta x & (\text{for } x > x_{MIN}) \end{cases}$$

for the case of $\beta = 0°$, and

$$E_{H\alpha}(\lambda) = 2\int_0^{\frac{x}{\tan\alpha_M}} \int_{-\infty}^{+\infty} 4\pi j_{H\alpha}\{n_c' e^{-(\frac{h}{H})^2}\}^2 \, dh\, dy\, \Delta x$$

for the case of $\beta = 90°$, where $x = c\Delta\lambda/(\Omega\lambda)$ if $\Delta\lambda$ is a wavelength shift from the line center, and Δx is the width of emitting volume perpendicular to the line of sight corresponding to $\Delta\lambda_{th}$. In the case of $\beta = 90°$, the circumstellar gas is on the plane perpendicular to the line of sight. Figure 6 shows the calculated Hα emission profiles. We find from the figure that the emission is fairly broad in the case of $\beta = 0°$, and shifts far from the line center in the case of $\beta = 90°$.

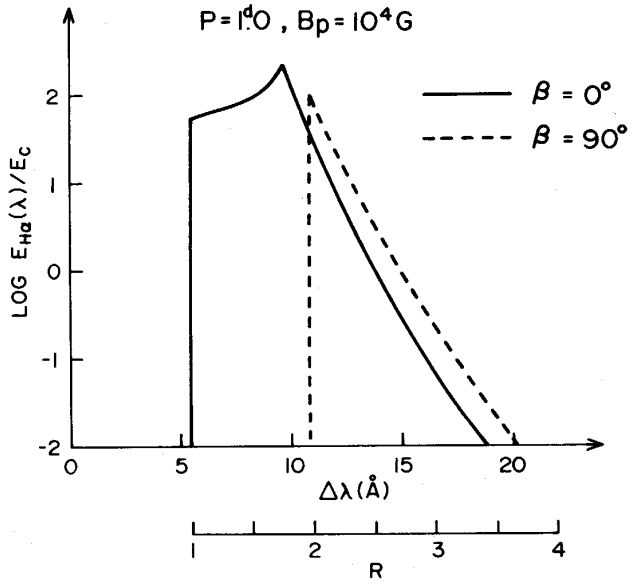

Fig. 6. The Hα emission profiles for $Bp = 10^4$ gauss and $P = 1.^d0$. The ordinate is an intensity in units of the stellar continuous radiation and the abscissa is a wavelength shift from the line center.

§5. Comparison with Observations and Conclusions

We found in section 4 that the Hα emission is negligible for $P = 10.^d0$. As the maximum critical density of the outer region decreases with $P^{-10/3}$, we conclude that the Hα emission appears only in short period stars. Indeed, the Hα emission is not observed in long period stars.[6)]

The Hα emission strength in σ Ori E is the largest of helium-rich stars with the Hα emission. As the rotation period of σ Ori E is $1.^d19$ and the lower limit of Bp of this star is 10^4 gauss,[4)] we can compare the observational results of Hα emission of σ Ori E with this model of $P = 1.^d0$. In σ Ori E, the Hα emission is observed to rise to at most about 10 % above the stellar continuum, and its maximum width is about 40 Å.[2,22)] Figure 6 shows that this model is consistent with the observations. Especially, it is important for this model that the amount of gas trapped in the outer region may be lower

than that for the critical density distribution, as we can infer that the magnetic field is nearly dipolar.

As the two trapping regions occur symmetrically about the star except for the case of small β, the emission appears in the both wings of Hα absorption line. However, if the amount of gas of the both regions are different from each other, the emission strength in one wing will not be equal to that in the other (e.g. HD 37017, σ Ori E, HD 64740), and also it will be possible that the emission appears only in either wing (e.g. HD 37776). Furthermore, the Hα emission will not appear if the magnetic field is so weak that it can scarcely contain gas.

This model explains naturally that the emission strength varies periodically except for the case of small β, if the circumstellar gas is hidden by the star with its rotation. In such a case, the emission strength becomes maximum at the phases of the extreme of magnetic field strength. This agrees with the observational results of σ Ori E (see Fig. 7).

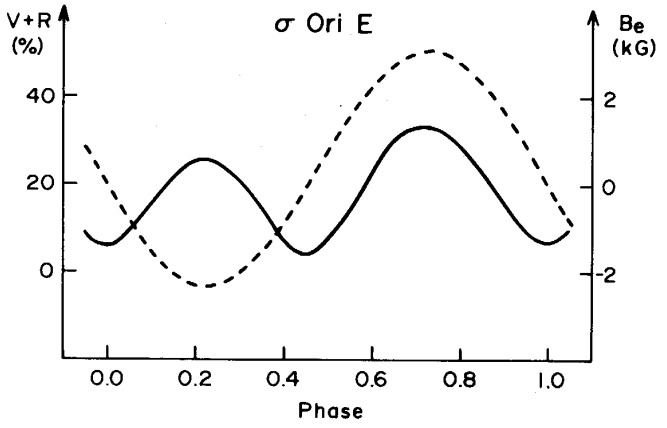

Fig. 7. The solid line shows the V + R,[22] where V and R are the percentage heights of the violet and red sides of the emission above the continuum, respectively. The dashed line shows the effective magnetic field.[4] The former line is handdrawn and the ordinate is a phase.

Finally, in this model, the circumstellar gas can also behave as an absorbing volume if it occults a stellar disk. Therefore, this model will explain the variations of the IR excess,[8] the number of the last resolved Balmer line,[23] the radial velocity of the additional Balmer lines,[24] and the brightness[25] of σ Ori E.

I am indebted to Dr. M. Takeuti for constant guidance and great encouragement in the course of the work. I am also grateful to Dr. O. Kaburaki for reading the manuscript carefully.

References

1) H. Pedersen and B. Thomsen: Astron. Astrophys. Supple. 30 (1977) 11.
2) H. Pedersen: Astron. Astrophys. Supple. 35 (1979) 313.
3) P.S. Osmer and D.M. Peterson: Astrophys. J. 187 (1974) 117.

4) J.D. Landstreet and E.F. Borra: Astrophys. J. Letters 224 (1978) L5.
5) E.F. Borra and J.D. Landstreet: Astrophys. J. 228 (1979) 809.
6) N.R. Walborn: Astrophys. J. Letters 191 (1974) L95.
7) D.F. MacConnell, R.L. Frye and W.P. Bidelman: Publ. Astron. Soc. Pacific 83 (1970) 730.
8) D. Groote, K. Hunger and G.V. Schultz: Astron. Astrophys. Letters 83 (1980) L5.
9) E.F. Borra and J.D. Landstreet: Astrophys. J. Supple. 42 (1980) 421.
10) M. Schwarzschild: Astrophys. J. 112 (1950) 222.
11) L.B. Lucy and P.M. Solomon: Astrophys. J. 159 (1970) 879.
12) T.P. Snow and D.C. Morton: Astrophys. J. Supple. 32 (1976) 429.
13) O. Havnes and P.S. Conti: Astron. Astrophys. 14 (1971) 1.
14) O. Havnes: Astron. Astrophys. 32 (1974) 161.
15) J.J. Angerami and J.O. Thomas: J. Geophys. Res. 69 (1964) 4537.
16) R. Nakajima: Sci. Rep. Tôhoku Univ. Ser.I 62 (1979) 35.
17) L. Spitzer: Physics of Fully Ionized Gases (Interscience Publications, New York 1962).
18) D. Chadeau: Compt. Rend. 250 (1960) 2130.
19) D.E. Osterbrock: Astrophysics of Gaseous Nebulae (Freeman, San Francisco 1974).
20) D. Mihalas: Astrophys. J. Supple. 9 (1965) 321.
21) V.V. Sobolev: in Theoretical Astrophysics ed. by V.A. Ambartsumian (Pergamon Press, New York 1958) P.478.
22) N.R. Walborn and J.E. Hesser: Astrophys. J. Letters 205 (1976) L87.
23) D. Groote and K. Hunger: Astron. Astrophys. 52 (1976) 303.
24) D. Groote and K. Hunger: Astron. Astrophys. 56 (1977) 129.
25) J.E. Hesser, N.R. Walborn and P.P. Ugarte: Nature 262 (1976) 116.